Cell

Cep97 and CP110 Suppress a Cilia Assembly Program

Alexander Spektor,[1] William Y. Tsang,[1] David Khoo,[1] and Brian David Dynlacht[1,*]
[1]Department of Pathology and NYU Cancer Institute, New York University School of Medicine, Smilow Research Center, 522 First Avenue, New York, NY 10016, USA
*Correspondence: brian.dynlacht@med.nyu.edu
DOI 10.1016/j.cell.2007.06.027

SUMMARY

Mammalian centrioles play a dynamic role in centrosome function, but they also have the capacity to nucleate the assembly of cilia. Although controls must exist to specify these different fates, the key regulators remain largely undefined. We have purified complexes associated with CP110, a protein that plays an essential role in centrosome duplication and cytokinesis, and have identified a previously uncharacterized protein, Cep97, that recruits CP110 to centrosomes. Depletion of Cep97 or expression of dominant-negative mutants results in CP110 disappearance from centrosomes, spindle defects, and polyploidy. Remarkably, loss of Cep97 or CP110 promotes primary cilia formation in growing cells, and enforced expression of CP110 in quiescent cells suppresses their ability to assemble cilia, suggesting that Cep97 and CP110 collaborate to inhibit a ciliogenesis program. Identification of *Cep97* and other genes involved in regulation of cilia assembly may accelerate our understanding of human ciliary diseases, including renal disease and retinal degeneration.

INTRODUCTION

Centrosomes are comprised of two perpendicularly oriented centrioles surrounded by a pericentriolar matrix from which microtubules emanate and elongate. Centrioles are cylindrical structures composed of specially modified, stable forms of tubulins (Edde et al., 1990). Many aspects of centriolar structure and function remain poorly understood, and only a small number of centriolar proteins have been described to date. In addition to their role in centrosome function, centrioles act as basal bodies that nucleate assembly of cilia or flagella, which are found in nearly all mammalian cell types (Quarmby and Parker, 2005; Wheatley et al., 1996). While motile cilia present in certain tissue types, such as lung epithelia, have been studied extensively in the past, recent evidence has pointed to the importance of the nonmotile primary cilium as an essential transducer of several critical signaling pathways.

Primary cilia are sensory antenna-like organelles that emanate from the cell surface of nearly all quiescent mammalian cells. They are capable of sensing a variety of chemical and mechanical signals from the cell environment in order to elicit proper physiological responses. Recent studies have implicated these organelles in pathways with well-established roles in embryonic development and tumorigenesis, including Sonic hedgehog (Shh) and platelet-derived growth factor receptor α (Reviewed in Michaud and Yoder, 2006). Strikingly, recent proteomic analyses indicate that many components of basal bodies of the green alga *Chlamydomonas reinhardtii* are extensively conserved in human centrioles, and a number of these basal body proteins are orthologous to mammalian genes implicated in ciliary function and disease (Keller et al., 2005). A similar conclusion was reached in the proteomic analysis of isolated human centrosomes (Andersen et al., 2003). Deficiencies in several of the genes encoding these human proteins give rise to a panoply of developmental defects and ciliary diseases, including renal dysfunction, diabetes, and retinal degeneration, although mechanistic details regarding the function of these proteins are completely lacking (reviewed in Badano et al., 2006).

Interestingly, mammalian centrioles function as basal bodies by nucleating cilia in a number of cell types that have become quiescent and have differentiated along certain developmental lineages (Sorokin, 1968; Wheatley et al., 1996). Moreover, there is evidence that most known cell types resorb their cilia either upon cell cycle re-entry or prior to entry into mitosis in order to allow centrosomes to participate in establishing spindle poles, thus ensuring accurate segregation of chromosomes (Rieder et al., 1979; Wheatley et al., 1996). Controls must exist to limit the capacity of centrioles to function either in the context of centrosomes (microtubule organizing centers) or as basal bodies that nucleate cilia. However, the mechanisms underlying the switch between centriolar and basal body function are completely unknown.

Much progress has been made toward understanding the complexity of mammalian centrosomes using proteomic analyses, which identified several hundred

polypeptides (Andersen et al., 2003). Although many of these proteins remain uncharacterized, several proteins essential for the proper function of centrosomes have been analyzed in detail. Using RNA interference (RNAi), several laboratories have demonstrated that the loss of a number of centrosomal proteins has detrimental effects on centrosome reproduction and cytokinesis (Gromley et al., 2003; Salisbury et al., 2002; Zhao et al., 2006; Zou et al., 2005). We identified a centrosomal protein (CP110) that interacts with two small calcium-binding proteins, calmodulin (CaM) and centrin, in vivo (Chen et al., 2002; Tsang et al., 2006). Depletion of CP110 or expression of mutants that are unable to bind CaM or that are refractory to CDK phosphorylation exhibit cytokinesis defects (Chen et al., 2002; Tsang et al., 2006). Furthermore, loss of CP110 results in premature centrosome separation and abrogates centrosome reduplication in S phase arrested cells (Chen et al., 2002).

Given the complexity of mammalian centrosomes and the dynamic maneuvers in which they are engaged, much work will be needed to understand how proteins such as CP110 interact to regulate the assembly and function of centrosomes or primary cilia. Here, we biochemically purified proteins that interact with CP110 and identified a previously uncharacterized protein, Cep97, that appears to functionally collaborate with CP110. Cep97 and CP110 share a number of properties indicative of a functional complex: loss of either protein results in aberrant mitotic spindles and cytokinesis defects. Remarkably, RNAi-mediated suppression of the Cep97-CP110 pathway results in the assembly of primary cilia in proliferating cells. Conversely, expression of CP110 robustly inhibits primary cilium formation in quiescent cells. Thus, *Cep97* and *CP110* represent the first genes shown to actively suppress assembly of cilia. Cep97 and CP110 could represent components of the switching mechanism that ensures the timely transition from centriolar to basal body function.

RESULTS

Biochemical Purification of CP110 Complexes

In previous work, we used a yeast two-hybrid screen to identify calmodulin (CaM) as a tight-binding partner of CP110, and we subsequently identified a second small calcium-binding protein, centrin, that interacted with CP110 indirectly (Tsang et al., 2006). Size exclusion chromatography indicated that native CP110 exists in very large complexes with a mass of 300 kDa to 3 MDa (Tsang et al., 2006), suggesting the likelihood of multiple CP110-interaction partners. We developed a biochemical purification scheme for the isolation of native CP110 containing complexes in which we fused a Flag epitope tag to the amino-terminus of full-length CP110 and immunopurified associated proteins (Figure 1), and several criteria indicated that this approach would reliably identify physiologically relevant interacting proteins (see the Supplemental Experimental Procedures in the Supplemental Data available with this article online).

After immunoaffinity purification of Flag-CP110, we eluted the resulting CP110-associated proteins with a Flag peptide, fractionated the eluate by SDS-PAGE (Figure 1A), and excised gel fragments which we subjected to proteolytic digestion and mass spectrometric (MS) sequencing. MS sequencing identified at least five known centrosomal and/or spindle pole proteins, including calmodulin (CaM). Interestingly, we identified several uncharacterized components identified in a recent proteomic analysis of isolated human centrosomes (Andersen et al., 2003), and these will be described elsewhere. Here, we describe the characterization of one component (*l*eucine-*r*ich *r*epeats and *IQ* motif containing *2*, or *LRRIQ2*; accession number NM_024548) identified in both our study and the proteomic analysis. We have renamed this protein Cep97 based on its centrosomal localization and predicted molecular weight (see below).

Cep97 encodes an uncharacterized protein of 865 amino acids with multiple leucine-rich repeats (LRR), an IQ CaM-binding motif, and a short coiled-coil domain (Figure 1B). Interestingly, homology searches revealed striking similarity to centriolin, a centriolar protein required for cytokinesis (Gromley et al., 2003), throughout the *Cep97* open reading frame but particularly over an amino-terminal region (E = e-8). The open-reading frame encoded by *Cep97* predicts a ~97 kDa protein, although the protein migrates at a molecular weight of approximately 140 kDa. We note that the protein is highly acidic, with a pI ~4.7, providing a potential explanation for its reduced mobility (and that of recombinant derivatives) in SDS-PAGE. We confirmed the interaction between Cep97 and CP110 by ectopically expressing Flag-tagged Cep97 and immunoprecipitating this protein using antibodies against CP110 (Figure S1B). Similarly, anti-Flag antibodies coprecipitated both Cep97 and CP110. In addition, Cep97 associates with CaM, an observation anticipated by the presence of an IQ domain. To determine whether Cep97 and CP110 directly interact, we in vitro translated both proteins and performed CP110 immunoprecipitations, which resulted in very efficient recovery of both proteins, suggesting that the proteins most likely interact directly (Figure 1C). Since both CP110 and Cep97 are CaM-binding proteins, we tested the possibility that the CP110-Cep97 interaction was mediated by CaM in the reticulocyte lysate by performing in vitro binding assays with CP110 mutants harboring small deletions that abrogate CaM association (Tsang et al., 2006). These studies suggested that CaM was not required to bridge interactions between Cep97 and CP110, and likewise, Cep97 mutants that do not bind CaM retain the ability to interact with CP110 (Figure 1C, and data not shown).

Characterization of Cep97

We raised a polyclonal antibody against Cep97 to study the endogenous protein (Figure 1D) and detected the

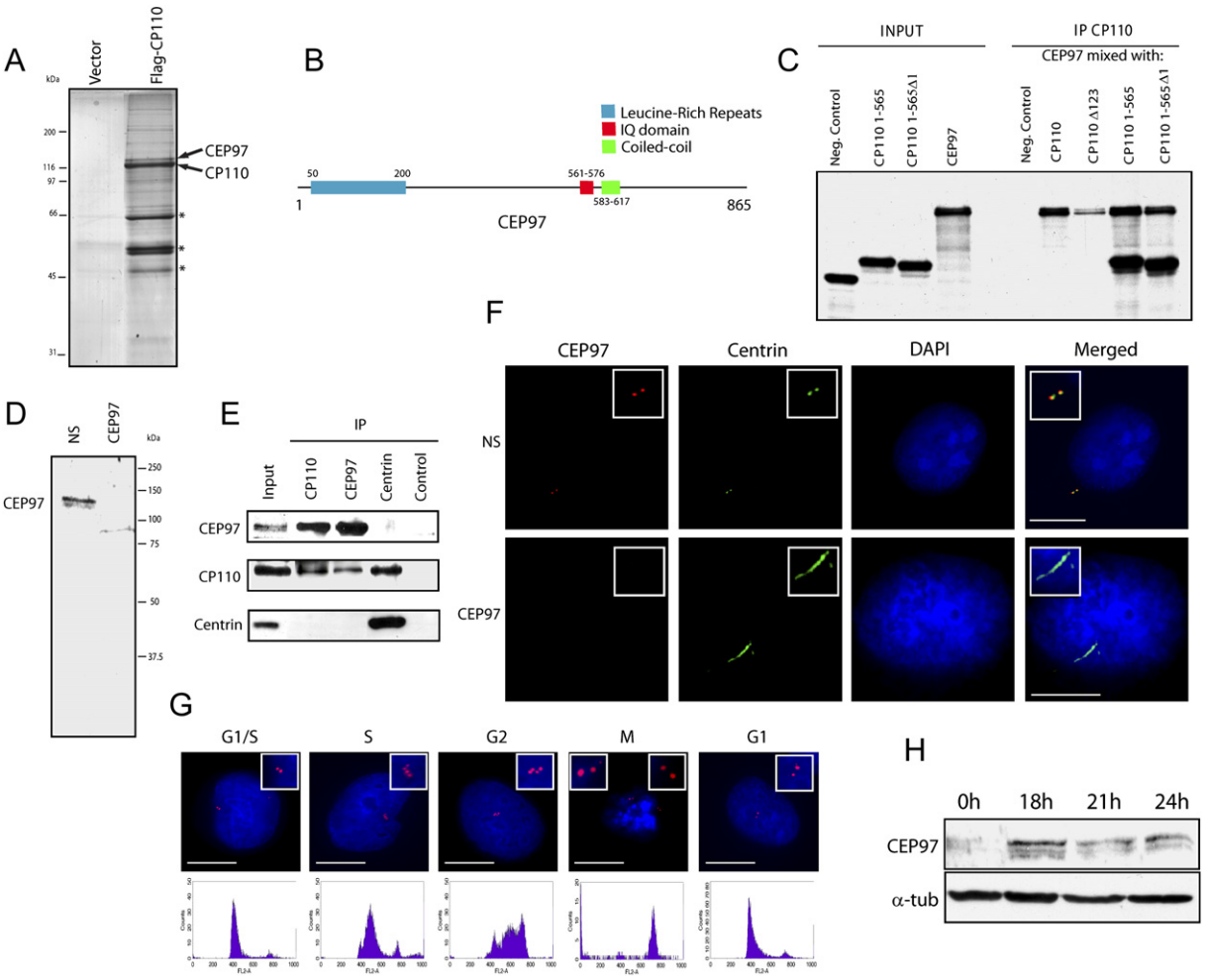

Figure 1. Identification of the CP110-Interacting Protein, Cep97

(A) Eluates from representative Flag-CP110 and control (vector) immunoaffinity purification experiments were silver stained and subjected to mass spectrometric sequencing. Silver stained gel represents 20% of total purified material. Assignment of Cep97 and CP110 was based on mobility of recombinant proteins and abundance of MS spectra. Contaminating bands observed in the control are indicated with an asterisk (*).

(B) Schematic of Cep97 domains.

(C) CP110 and Cep97 interact, most likely directly. Cep97, full-length CP110, an N-terminal fragment of CP110 containing the first 565 residues (CP110 1-565), and CP110 mutants unable to bind CaM (CP110Δ123 and CP110 1-565Δ1) were translated in vitro using reticulocyte lysates, and the resulting ^{35}S-methionine labeled proteins were detected by autoradiography before and after immunopreciptation. Since full-length CP110 and CEP97 have similar electrophoretic mobility, full-length CP110 was not labeled with ^{35}S-methionine; all other proteins were labeled. Full-length CP110 expression was confirmed by immunoblotting (data not shown).

(D) Western blot detection of endogenous Cep97 with affinity-purified anti-Cep97 antibodies. Cells were transfected with a nonspecific control (NS) and Cep97-specific siRNAs as indicated (top). Endogenous Cep97 is indicated (left).

(E) Endogenous Cep97 and CP110 interact in vivo. Cep97 and CP110 were immunoprecipitated with their respective antibodies, and both proteins were also observed in reciprocal reactions. CP110 appears to associate with discrete complexes, since centrin antibody immunoprecipitates CP110, but not Cep97, and Cep97 antibodies immunoprecipitate CP110 but not centrin.

(F) Cep97 localization to centrosomes and specificity of Cep97 antibodies. (Top) Immunofluorescent detection of Cep97 (red) in cells transfected with NS (top) or Cep97-specific (bottom) siRNA. Cep97 staining overlapped with centrin (green).

(G) Cep97 is expressed and localizes to centrosomes throughout the cell cycle. U2OS cells were synchronized with a double thymidine block, released for 0, 3, 8, 11, and 14 hr, and stained for Cep97. Cell cycle distribution was monitored by FACS analysis (bottom).

(H) Cep97 is expressed at substantially reduced levels in G0. T98G cells were synchronized by serum starvation and re-stimulated for indicated times. Cep97 and α-tubulin expression were determined by immunoblotting. Cell cycle distribution was confirmed by FACS (data not shown).

protein in lysates from several different human cell lines. To further document the specificity of this antibody, we screened small interfering RNA (siRNA) pools targeting Cep97 for the ability to deplete the protein recognized on immunoblots. Treatment of cells with two distinct pools of siRNAs depleted ~80%–90% of Cep97, and two unique siRNAs derived from these pools performed similarly (Figure 1D, and data not shown).

To determine whether CP110 and Cep97 interact in vivo, we performed immunoprecipitations with affinity-purified CP110 and Cep97 antibodies. Both CP110 and Cep97 were immunoprecipitated by CP110 antibodies, and reciprocal immunoprecipitations with Cep97 antibodies confirmed this physiological interaction (Figure 1E). CP110 has been shown to associate with both CaM and centrin, and we therefore tested the ability of Cep97 to interact with a similar cohort of proteins. Although we readily detected CP110 in centrin immunoprecipitates, as expected (Tsang et al., 2006), we did not observe Cep97. Moreover, Cep97 failed to immunoprecipitate centrin, although CP110 and CaM were detected (Figure 1E, and data not shown), suggesting that CP110 associates with discrete centrin and Cep97 complexes.

We examined the subcellular localization of Cep97 by performing immunofluorescence experiments with our affinity-purified antibody. Endogenous Cep97 localized exclusively to centrosomes, consistent with its ability to interact with CP110, and Cep97-GFP (tagged on the carboxy-terminus) showed similar localization (Figure 1F, top panel and data not shown). Moreover, Cep97 staining overlapped extensively with centrin, a canonical centriolar protein, suggesting that Cep97 colocalizes with CP110 at centrioles. Centrosomal localization of Cep97 was not affected by treatment with nocodazole, a microtubule depolymerizing drug, indicating that Cep97 is an intrinsic component of centrosomes (data not shown). Importantly, transfection of a Cep97 siRNA completely abolished the appearance of Cep97 at centrosomes, confirming the specificity of our antibodies and Cep97 centrosomal localization (Figure 1F, bottom panel). Strikingly, we observed an abnormal distribution of centrin in Cep97 depleted cells, which we subsequently investigated (Figures 1F and 2C, and see below). Next, we examined whether Cep97 associates with centrosomes in a cell cycle-dependent manner by synchronizing cells and enriching for stage-specific populations. This analysis suggested that Cep97 partitions to centrosomes irrespective of cell cycle status (Figure 1G). In order to test the expression of Cep97 in G0, we synchronized T98G cells by serum starvation, and we observed a substantial decrease in Cep97 levels in these cells (Figure 1H).

Cep97 Is Required for Recruitment of CP110 to Centrosomes

We determined the consequences of knocking down Cep97 expression by examining the expression and localization of CP110 in cells transfected with siRNAs targeting Cep97. We transfected two distinct siRNAs and showed that expression of Cep97 was routinely and dramatically reduced by ~80%–90% using RT-PCR and Western blotting (Figure 2A and 2B). Flow cytometric analysis indicated that suppression of Cep97 did not alter cell cycle progression (data not shown). Interestingly, depletion of Cep97 led to the disappearance of CP110 from centrosomes (Figure 2C, top panel, and Figure 2D), and Western blotting indicated that total CP110 levels were significantly reduced (Figure 2B). We also performed the converse experiment in which we suppressed expression of CP110 using RNAi and determined whether Cep97 levels were affected. Depletion of CP110 led to the disappearance of Cep97 from centrosomes (Figure 2C bottom panel and 2E), although Cep97 expression was not globally altered (Figure 2B). These data suggest that Cep97 and CP110 are coordinately recruited to centrosomes and that Cep97 is required to stabilize CP110 protein.

Cep97 Depletion Results in Abnormal Mitotic Spindles and Cytokinesis Defects

Next, we examined a role for Cep97 in centrosome function. We used an siRNA to deplete Cep97 from U2OS cells and observed several notable defects suggesting that centrosome function had been compromised. First, we observed a striking increase in the number of cells with abnormal mitotic spindles in Cep97-depleted cells as compared to controls (Figure 3A). Notably, the number of cells with monopolar and multipolar spindles increased markedly in cells lacking Cep97. Moreover, some of the cells with abnormal mitotic spindles exhibited a striking microtubular structure that emanated from centrosomes and contained acetylated tubulin (Figure 3A). We asked whether additional abnormalities could result from these spindle defects after Cep97 depletion and observed a significant increase in the number of binucleate cells, suggesting that cytokinesis was defective in these cells (Figure 3B). Importantly, both of these phenotypes were independently observed with a second, unique siRNA targeting Cep97 (Figure 3B and data not shown). Similar phenotypes were observed in cells depleted of CP110 (Tsang et al., 2006), and they reinforce the notion that Cep97 collaborates with CP110 to regulate a subset of essential centrosomal functions.

Cep97 and CP110 Depletion Provokes Inappropriate Assembly of Cilia

Our data suggested that Cep97 plays an important role in centrosome function. To understand how the loss of Cep97 could give rise to centrosome abnormalities, we examined the localization of several well-established centrosomal markers after depleting Cep97 in an effort to determine whether the apparent defects might be ascribed to improper localization of proteins instrumental for its function.

First, we examined centrin staining in cells transfected with control siRNAs or duplexes targeting the *Cep97* gene. In normal and control cells, anti-centrin antibodies stain centrioles, resulting in the appearance of two dots in cells that have not replicated their centrosomes and four dots after reproduction of the organelle, as expected (Figure 4A). Remarkably, cells depleted of Cep97 exhibited radical alterations in the appearance of centrin: instead of dots, centrin appeared in long filamentous structures (Figure 4A). In some instances, these filaments extended several microns in length, surpassing the breadth of an entire centrosome and subtending half

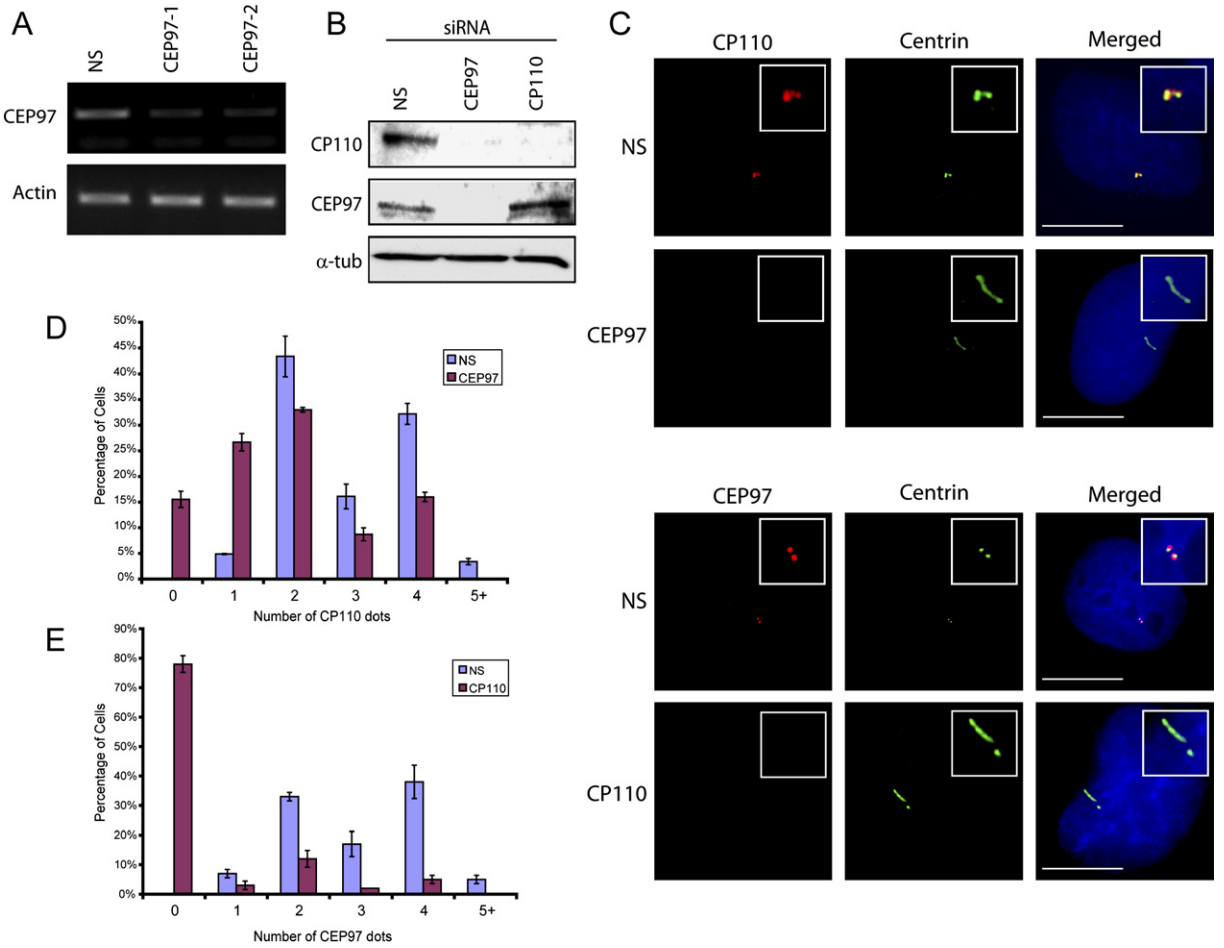

Figure 2. Cep97 and CP110 are Corecruited to Centrosomes

(A) and (B) Depletion of Cep97 with two siRNAs (indicated at top) was assessed by (A) RT-PCR and (B) Western blotting. Cep97 and CP110 expression in reciprocal knock-downs was assayed. These experiments indicated significant reduction in CP110 levels in both CP110 and Cep97 siRNA-treated U2OS cells. α-tubulin loading and specificity controls are shown. (C) and (D) RNAi-mediated Cep97 depletion results in disappearance of CP110 from centrosomes (C, top panels). (C) U2OS Cells were stained with the indicated antibodies (top). Disappearance of CP110 dots from centrosomes was quantitated and is shown in the histogram (D). (C) and (E) CP110 depletion results in the disappearance of Cep97 from centrosomes (C, bottom panels) but not cell extracts (B). Disappearance of Cep97 dots from centrosomes was quantitated and is shown in the histogram (E).
In all cases, scale bars are equivalent to 10 μm, and error bars represent ± standard deviation (SD).

the diameter of a nucleus. Importantly, we have also observed similar centrin filaments using a second, distinct Cep97 siRNA or two pools of siRNAs containing nonoverlapping sets of Cep97 siRNAs (data not shown). In addition, we observed centrin filaments in a second human (T98G) cell line (data not shown). The appearance of filaments was not cell cycle-specific, since they persisted from G1 phase into mitosis (Figure 3A). Interestingly, we noted that in the majority of cells, these centrin filaments primarily extended from a single centriole, although occasionally, we observed the filaments emanating from two centrioles (data not shown). We have further detected an abnormal distribution of γ-tubulin, a centriolar and pericentriolar matrix (PCM) protein that is required for nucleation of microtubules, in Cep97 knockdown cells (Figures S3 and 4B–4E). Despite the abnormal γ-tubulin staining in Cep97-depleted centrosomes, no overt defect was observed in microtubule nucleation experiments performed in nocodazole-treated cells, nor did we observe such dramatic differences in the appearance of a second PCM protein, CG-NAP (data not shown).

In light of the in vivo association between Cep97 and CP110 and the apparent functional relationships between these proteins, we examined γ-tubulin and centrin staining after depleting CP110 with RNAi. We observed both abnormal γ-tubulin staining and centrin filaments in CP110-depleted cells, similar to the Cep97 phenotype (Figures 4A and S3). These data further suggest that Cep97-CP110 complexes are physically and functionally linked and are required for assembly of normal centrosomes.

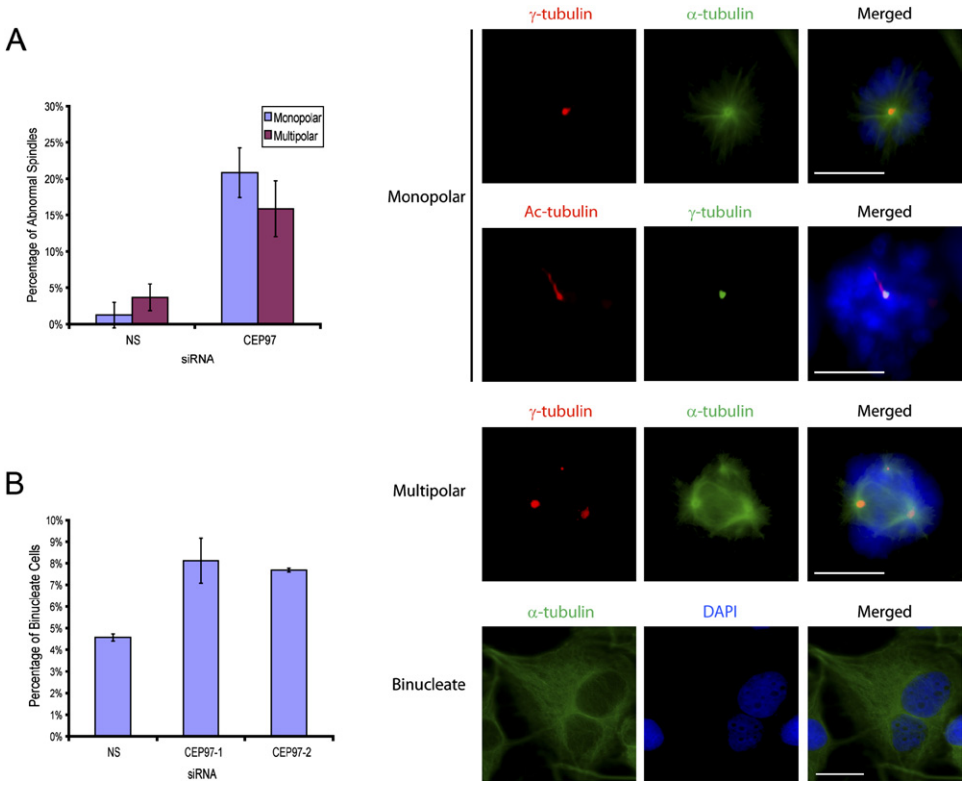

Figure 3. Phenotypic Consequences of Cep97 Knockdown

(A) Transfection of Cep97 siRNAs results in abnormal mitotic spindle assembly. U2OS cells were transfected with nonspecific control (NS) or Cep97 siRNAs as indicated. (Right) Representative cells with monopolar and multipolar spindles and (left) histogram quantifying these defects.

(B) Depletion of Cep97 results in formation of binucleate cells. Results were quantitated and are shown in the histogram. Representative images of a cell in nonspecific control (NS) and Cep97 knockdown (Cep97) populations are shown (right). Scale bars are equivalent to 10 μm. Error bars represent ± SD.

To address whether centriolar structure was altered or whether the defects were restricted to centrin alone, we examined additional centriolar proteins, polyglutamylated tubulins and C-Nap1. In contrast with centrin, which is primarily localized within the distal lumen of centrioles, polyglutamylated tubulins comprise the microtubule scaffold (Bobinnec et al., 1998). Interestingly, polyglutamylated tubulin appeared to precisely colocalize with extended centrin filaments in cells depleted of either Cep97 or CP110 but not the corresponding controls (Figure 4B). These results suggest that the centriolar defects provoked by loss of either protein are not restricted to centrin.

We also examined C-Nap1 in cells transfected with control and Cep97 siRNAs. Remarkably, the distribution of C-Nap1 was not altered in cells depleted of Cep97, and a single dot was observed at each centriole in control, Cep97, and CP110 siRNA transfected cells (Figure 4C). Since C-Nap1 localizes primarily to the proximal end of the centriolar cylinder (Fry et al., 1998), our results suggest that loss of Cep97 causes specific and local perturbation of the distal portion of centrioles.

The strikingly long, aberrant filaments emanating from centrioles were reminiscent of primary cilia. Primary cilia originate from the distal region of centrioles (basal bodies) in a number of mammalian cell lines that have entered quiescence and/or differentiated into various lineages. These structures often exhibit narrowing at the tip of the axoneme. Cilia typically originate from the mother centriole, and our observation of filaments emanating primarily from the distal region of a single centriole supported this hypothesis. Furthermore, C-Nap1 protein, which is found in centrioles but not within the ciliary axoneme (Beisson and Wright, 2003), was not delocalized as a consequence of Cep97 loss. To further test this hypothesis, we examined cells for a well-established primary cilium marker, acetylated tubulin (Ac-tubulin), after transfection with control, Cep97, and CP110 siRNAs. Antibodies against Ac-tubulin weakly stained a subset of cytoplasmic microtubules in cells transfected with control siRNAs. Remarkably, robust cilia-like structures containing Ac-tubulin appeared in cells depleted of either Cep97 or CP110 (Figure 4D). These structures predominantly extended from a single centriole, although we occasionally observed cells with two structures (data not shown). To confirm that the Ac-tubulin staining marked stabilized microtubules rather than dynamic cytoplasmic microtubule networks, we

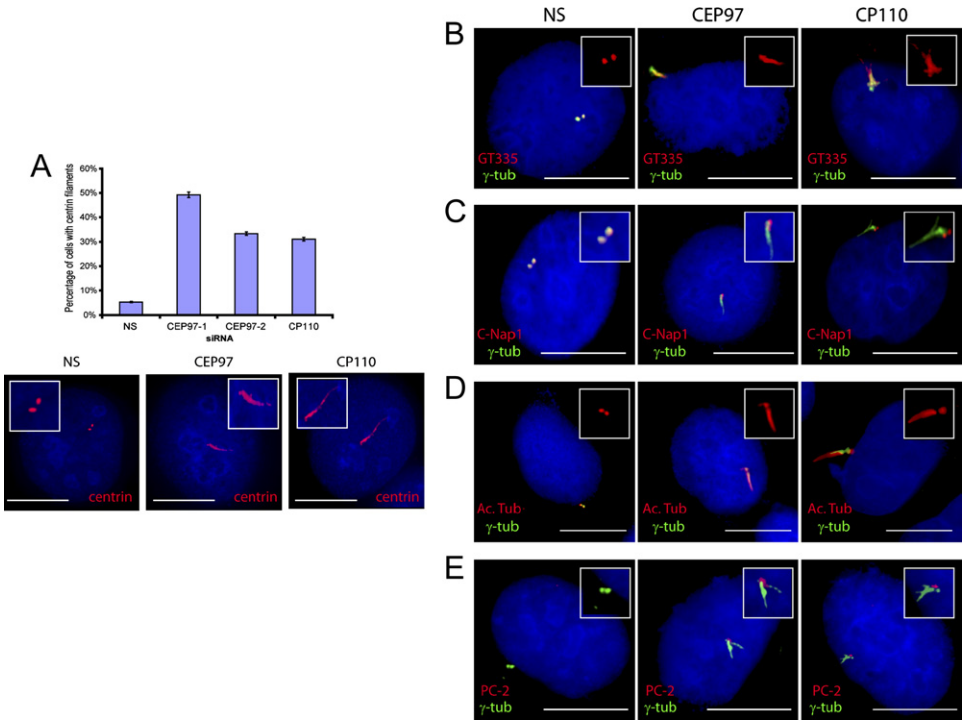

Figure 4. Depletion of CEP97 and CP110 Leads to Aberrant Outgrowth of Cilia from Distal Ends of Centrioles

(A) Aberrant centrin filaments form in the absence of Cep97 or CP110. Centrin was visualized in cells transfected with control, Cep97, and CP110 siRNAs, as indicated. Centrin filaments in a Cep97 knockdown persist into mitosis (top left). The centrin filament phenotype was quantitated, and results are shown in the histogram. Error bars represent ± SD.

(B) Abnormal centrosome filaments are composed of polyglutamylated tubulins. U2OS cells treated with indicated control, Cep97, and CP110 siRNAs were stained for polyglutamylated tubulin (GT335) (red) and γ-tubulin (green). DNA was stained with DAPI. Insets show a magnified view of polyglutamylated tubulin staining.

(C) C-Nap1 localization is not perturbed in U2OS cells depleted of Cep97 or CP110. C-Nap1 (red), which localizes to the proximal portion of centrioles, and γ-tubulin (green) are shown.

(D) Centrin filaments observed in Cep97- and CP110-depleted U2OS cells are composed of acetylated tubulin, indicative of primary cilia. Cells were treated with nocodazole for 1 hr to depolymerize cytoplasmic microtubules. Acetylated-tubulin (red) and γ-tubulin (green) were detected. Inset shows a magnified view of acetylated-tubulin signal.

(E) Polycystin-2 antibodies stain the filaments in Cep97 and CP110 knock-downs. Polycystin-2 (red) and γ-tubulin (green) were visualized. In all cases, scale bars are equivalent to 10 μm.

briefly treated Cep97- and CP110-depleted cells with nocodazole to depolymerize these microtubules. Drug treatment enhanced our ability to visualize stable microtubular structures morphologically resembling primary cilia emanating from centrosomes in cells lacking either Cep97 or CP110 (Figure 4D). In sharp contrast, cells transfected with nonspecific control siRNAs exhibited staining of a pair of centrioles of normal length and morphology.

As a further test, we examined a second marker for primary cilia, polycystin-2 (Cai et al., 1999). Cells that are depleted of Cep97 exhibited enhanced staining for this marker, reminiscent of previous studies of cilia (Pazour et al., 2002), in contrast to control transfected cells (Figure 4E). One explanation for our data is that primary cilia assemble in cells lacking Cep97 and CP110. To our knowledge, this phenotype—wherein loss of a protein gives rise to structures resembling primary cilia—has not been described previously. We suggest that loss of Cep97 or CP110 function relieves an inhibitory barrier, activating a switch that sets in motion a ciliary assembly program in proliferating somatic cells.

Our experiments strongly indicated that loss of Cep97 or CP110 resulted in inappropriate assembly of primary cilia. However, since the formation of this structure had not been documented in U2OS cells, we performed analogous experiments in other cell lines to substantiate our findings. It has been shown that murine 3T3 fibroblasts and human retinal pigment epithelial cells (RPE-1) readily develop primary cilia upon entry into a quiescent state provoked by mitogen deprivation or contact inhibition, and these are both well-established models for cilia formation (Ishikawa et al., 2005). We confirmed that both cell lines assemble bona fide primary cilia upon entry into a quiescent state, as expected, by staining for Ac-tubulin, polyglutamylated tubulin, and polaris, a protein known to localize to ciliary axonemes (Figure 5 and data not shown). More importantly, when we depleted either Cep97 or CP110 protein, we observed a consistent and

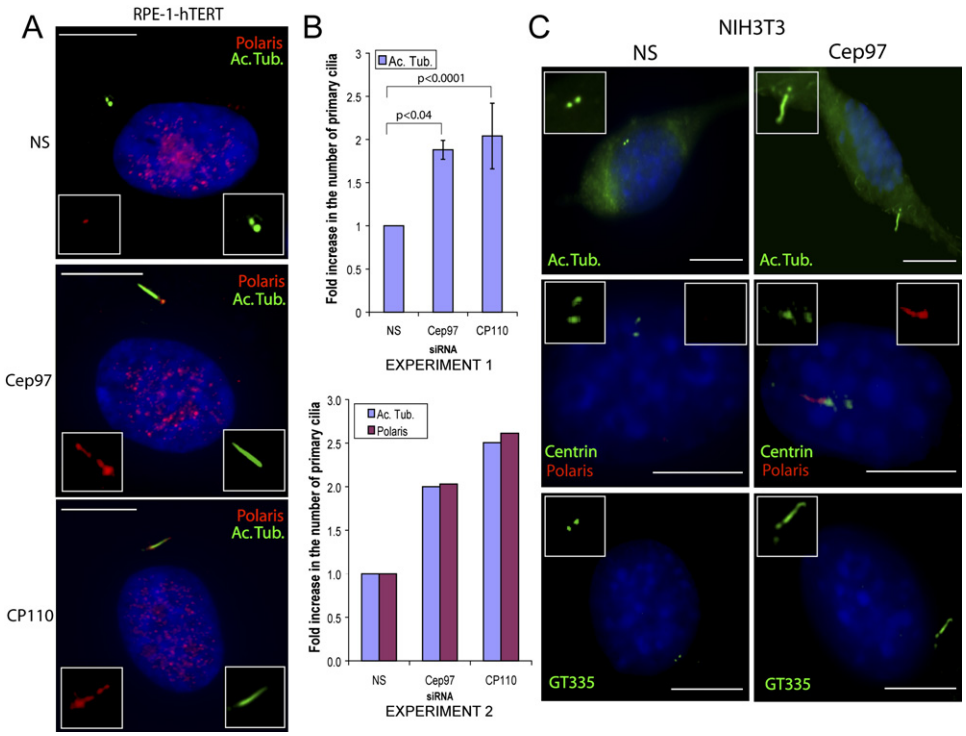

Figure 5. Induction of Cilia in RPE-1 and 3T3 Cells

(A) RPE-1 cells were transfected with the indicated siRNAs and stained with antibodies against Ac-tubulin and polaris as shown. Insets show each channel individually.

(B) Histograms quantifying the induction of cilia in RPE-1 cell line upon Cep97 and CP110 knockdown. Experiment 1 shows a summary of all studies performed with the Ac-tubulin marker. The average percentage of cells with primary cilia after transfection with NS siRNA was 10.3%. Experiment 2 presents quantitation of data using two ciliary markers, Ac- tubulin and polaris, in one individual experiment. For this experiment, the percentage of cells with primary cilia after transfection with NS siRNA was 11.0%. In each case, a minimum of 200 cells were scored per experiment. Error bars represent ± SD.

(C) 3T3 cells were transfected with the indicated siRNA pools and stained with antibodies against Ac-tubulin, polyglutamylated tubulin (GT335), centrin and polaris as shown. In all cases, scale bars are equivalent to 10 μm.

striking increase in the appearance of all ciliary markers in both RPE-1 (Figures 5A and 5B) and 3T3 (Figures 5C and S2) cells. FACS analysis indicated that the appearance of primary cilia was not precipitated by a G0/G1 cell cycle block (data not shown). These results provide conclusive evidence that Cep97 and CP110 are required to suppress ciliogenesis in both human and mouse cells.

Characterizing the Cep97-CP110 Interaction and Creation of Dominant-Negative Mutations

Our in vitro binding experiments suggested that Cep97 interacts, most likely directly, with CP110 (Figure 1), and therefore we sought to delineate the regions of each protein that enable this interaction with the hope of functionally dissecting Cep97. First, we determined which segments of CP110 interact with Cep97. We co-transfected human cells with Cep97-GFP and a series of Flag-tagged CP110 truncation mutants, and performed immunoprecipitations with anti-Flag antibodies. Cep97-GFP was readily detected on Western blots after immunoprecipitation of Flag-CP110, as expected (Figures 6A and 6B). We found that a fragment containing 223 amino-terminal residues was necessary and sufficient to bind Cep97 (Figure 6B). In addition, we tested whether a CaM-CP110 complex was essential for Cep97 interaction using mutants lacking high-affinity CaM-binding sites (Figure 1C; Tsang et al., 2006). We found that both an amino-terminal CP110 fragment and a full-length mutant incapable of binding CaM retained the ability to bind Cep97 (data not shown).

Next, we performed the reciprocal experiment to determine the regions of Cep97 involved in binding CP110. We constructed and transfected a set of Flag-tagged Cep97 amino- and carboxy-terminal truncation mutants and performed anti-Flag immunoprecipitation and Western blotting to detect endogenous CP110. We found that a region of Cep97 containing residues 300-750 was required for stable binding to CP110 (Figures 6C and 6D). In total, our data indicate that an amino-terminal region of CP110 directly interacts with residues in the middle and carboxy-terminal portion of Cep97.

We noticed that each of these Flag-tagged Cep97 fusion proteins, including full-length Cep97, failed to localize properly to centrosomes. This could be due to disruption

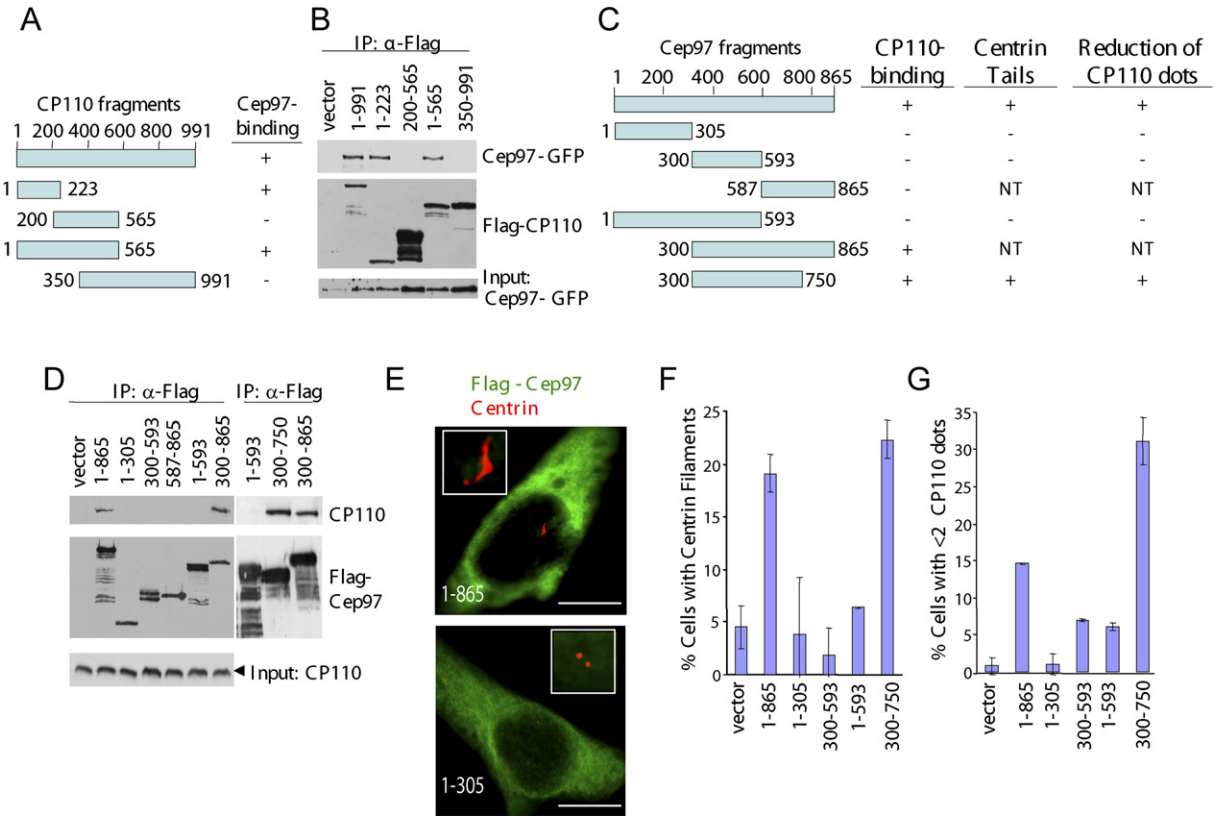

Figure 6. Mapping of Cep97-CP110 Interaction Surfaces and Identification of Dominant-Negative Cep97 Mutants

(A and B) Summary of CP110 truncation mutants and the results of in vivo binding experiments. (B) Cep97 interacts with an amino-terminal portion of CP110. The indicated fragments of Flag-tagged CP110 (top) were coexpressed with GFP-tagged Cep97 in 293 cells and immunoprecipitated from lysates. Flag-CP110 fusion proteins and GFP-Cep97 were detected after Western blotting the resulting immunoprecipitates. Input GFP-Cep97 was detected in lysates from each transfection (bottom).

(C) Summary of Cep97 truncation mutants and their properties, including binding to CP110, induction of primary cilia (scored as "centrin tails"), and disappearance of CP110 from centrosomes ("reduction of CP110 dots").

(D) (Top) The indicated Flag-tagged fragments of Cep97 (shown in panel [C] were expressed in 293 cells and immunoprecipitated with anti-Flag antibodies. Endogenous CP110 and each of the Cep97 fusion proteins were detected by immunoblotting as indicated.

(E and F) Ectopic expression of Flag-Cep97 mutants that are able to interact with CP110 induce aberrant cilium formation. Flag-Cep97 (green) and centrin (red) were visualized. Scale bars are equivalent to 10 μm. These data were quantitated and are shown in a histogram (F).

(G) Expression of Cep97 mutants that bind CP110 result in depletion of CP110 from centrosomes. In all cases, error bars represent ± SD.

of critical interactions with other centrosomal proteins stemming from fusion of the epitope-tag to the amino-terminus of Cep97, or it could result from elevated levels of Cep97 that surpass the limiting quantities of CP110, which we have shown to be required to recruit Cep97 to centrosomes (Figure 2C). These Cep97 fusion proteins nevertheless interacted stably with CP110, and we exploited this property to examine the effect of ectopically expressing each of these proteins in U20S cells. Remarkably, we observed two striking phenotypes reminiscent of Cep97 depletion in cells transfected with full-length Cep97, formation of centrin filaments and loss of CP110 from centrosomes (Figures 6E—6G). We note that expression of these fusion proteins gave rise to structures resembling cilia, although the phenotype was more pronounced in cells depleted of Cep97 (Figures 4 and 5). Importantly, both phenotypes absolutely depended on the ability of Cep97 to interact with CP110, since fusion proteins that were incapable of interacting with CP110 were unable to elicit either phenotype (compare deletions encoding residues 1-593 with one containing residues 300-750; Figure 6F, G). These results suggest that we have created dominant-negative mutants, and these experiments are significant because they employ methods that do not rely on RNAi to confirm the phenotypes observed with Cep97 and CP110 siRNAs. Furthermore, they reinforce the notion that CP110 localization to centrosomes is a sine qua non for normal assembly of centrioles and suppression of aberrant cilia formation.

Ectopic Expression of CP110 Suppresses Primary Cilia Formation in Quiescent Mammalian Cells

One hallmark of many quiescent cells is the ability to form primary cilia. We had previously shown that CP110 mRNA

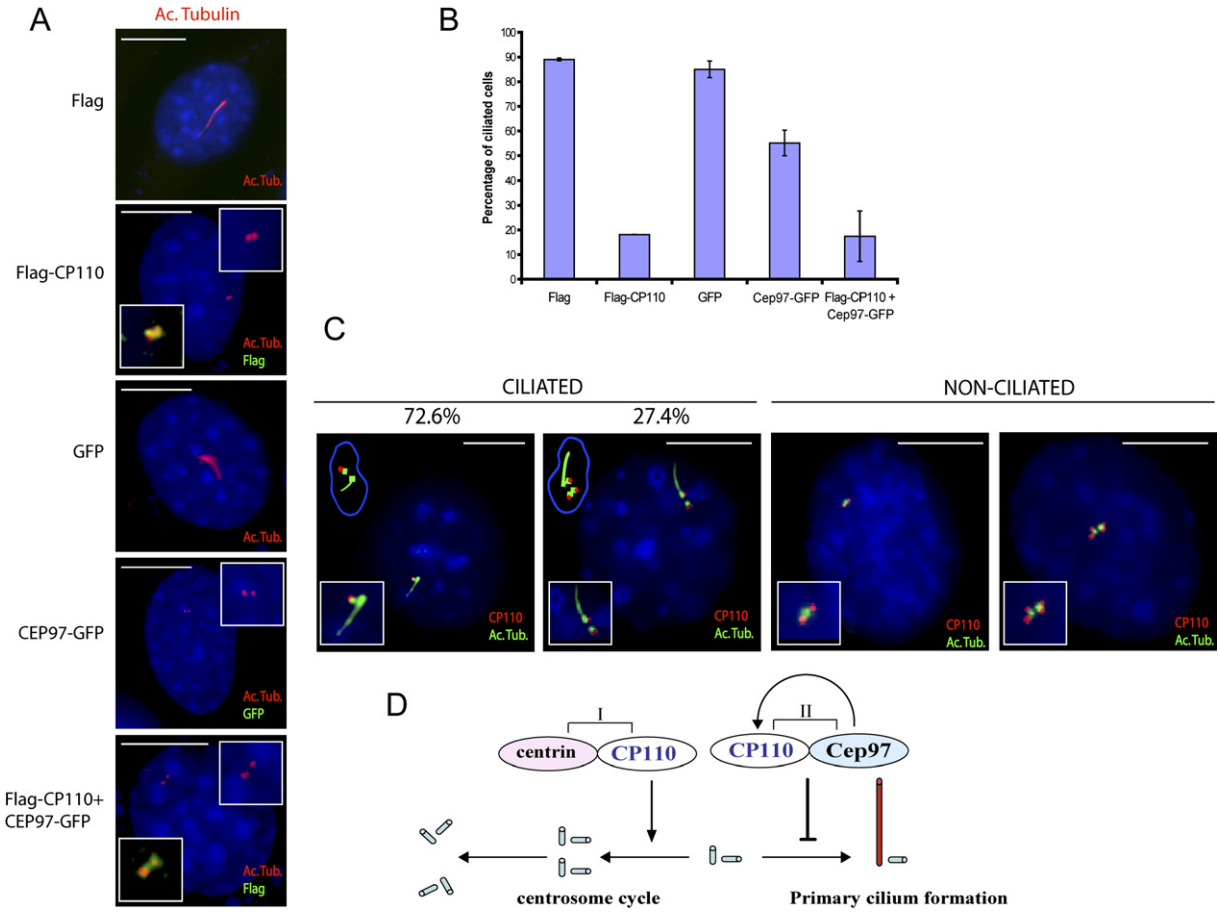

Figure 7. Suppression of Primary Cilia by Ectopic Expression of CP110 in Quiescent 3T3 Fibroblasts

(A and B) 3T3 cells were transfected with parental plasmids, Flag-tagged CP110, Cep97-GFP, or a combination of CP110 and Cep97 plasmids as indicated, and brought to quiescence by serum starvation. Control transfected cells and GFP transfected cells show evidence of typical primary cilia, whereas cells that overexpress CP110, Cep97 or a combination of both fail to assemble cilia or do so with reduced efficiency. Transfection was confirmed by staining for either GFP or Flag (insets). Representative images of acetylated-tubulin signal in successfully transfected (GFP+ or Flag+) cells are shown in (A). Insets show a magnified view of centrosomes or primary cilia. The percentage of GFP+ or Flag+ ciliated cells was quantitated in each overexpression assay and shown in (B). Error bars indicate +/− SD.

(C) Local disappearance of CP110 in untreated 3T3 cells is associated with outgrowth of cilia. Panels represent asynchronous, untransfected ciliated and nonciliated NIH 3T3 cells. In each case, the left panel shows a cell in G1, while the right panel shows a cell in S/G2. Percentage of cells falling into these two categories is as indicated above. Scale bars are equivalent to 10 μm.

(D) Model summarizing the function of two distinct CP110-containing complexes. See text for details.

and protein levels are barely detectable in quiescent cells, and they dramatically increase in cells that re-enter the cell cycle, peaking in S phase (Chen et al., 2002). We therefore speculated that CP110 might constitute part of a regulatory switch that suppresses cilia assembly at inappropriate times, i.e., during proliferation, and that its loss promotes the inappropriate formation of cilia in growing cells. If this hypothesis were correct, the absence of CP110 in quiescent cells might play an important functional role by allowing cells to assemble cilia during a permissive growth state. We tested this hypothesis by asking whether we could abolish formation of primary cilia in 3T3 cells that have been brought to quiescence. Cells were transfected with plasmids that express Flag-CP110, Cep97-GFP, or parental controls, brought to quiescence by serum starvation, and stained for the presence of Ac-tubulin. We confirmed expression and proper localization of each of these epitope-tagged proteins by immunofluorescence (Figure 7A). After 48 hr of serum starvation, most untreated cells and cells transfected with control plasmids expressed primary cilia (Figures 7A and 7B). In striking contrast, the majority of cells expressing Flag-tagged CP110 exhibited no cilia within 72 hr post-induction, suggesting that inappropriate expression of CP110 can suppress cilia assembly. A similar observation was made with cells expressing Cep97-GFP, although the effect was considerably less pronounced. Combined expression of Flag-CP110 and Cep97-GFP resulted in suppression of primary cilia to an extent comparable to that observed in Flag-CP110 transfected cells. We demonstrated that this

effect was not due to inappropriate cell cycle re-entry by staining with the Ki-67 proliferation marker and BrdU labeling (data not shown).

It has been shown that cilia can persist in cells that have re-entered the cell cycle, although the structure is normally resorbed prior to mitosis. We asked how this scenario could be compatible with expression of CP110. Remarkably, when we visualized primary cilia in growing 3T3 cells in G1 or subsequent stages of the cell cycle, we found that CP110 expression was specifically extinguished from the basal body that gives rise to a primary cilium, although it did not disappear from an adjacent centriole (Figure 7C). We did not observe a single instance in which CP110 protein was present at a basal body associated with a cilium, and we observed the same result in RPE-1 cells (not shown). These data, obtained from an unperturbed population of 3T3 cells, strongly suggest that local disappearance of CP110 at centrioles could be required to allow the transition from centriolar to ciliary assembly. Taken together with our ectopic expression experiments, we conclude that the absence of CP110 could create a "default state" permissive for assembly of cilia. Its absence may be obligatory for promoting this permissive state.

DISCUSSION

Phenotypes Associated with the Loss of Cep97 and CP110

Here, we have shown that depletion of Cep97 subverts normal centriolar function and leads to inappropriate formation of primary cilia. We suggest that one function of CP110-Cep97 complexes is to suppress assembly of cilia and that the phenotypes observed in this report, including the aberrant cilia formation, could explain the cytokinesis defects. Loss of Cep97 also phenocopies a number of the defects that were observed previously upon knocking down CP110, including spindle defects. However, additional studies will be required to definitively link the appearance of cilia and mitotic defects.

We speculate that CP110 might control discrete functions in the centrosome cycle: certain tasks could require centrin-containing complexes, whereas others might be executed through Cep97, which could stabilize CP110 (arrow, Figure 7D). Although we do not know precisely how many distinct CP110 complexes exist in vivo, the broad distribution of CP110 on gel filtration columns indicates that multiple high molecular weight complexes, consisting of additional proteins beyond those that we have already described, are likely to exist (Tsang et al., 2006). Our data suggest that at least two CP110 complexes with discrete functions might exist (Figures 1E and 7D): one complex, containing CP110 and centrin, may be important for centrosomal functions, including centrosome duplication and separation. A second complex, consisting of CP110 and Cep97 might be involved in regulating basal body function and assembly of primary cilia. These complexes may not exhibit mutually exclusive functions, but our data suggest that centrin and Cep97 reside in separate complexes, and loss of these proteins can be distinguished in specific assays. Indeed, we have found that loss of CP110, but not Cep97, leads to defects in centrosome duplication and premature centrosome separation (Chen et al., 2002 and data not shown).

Several observations support the conclusion that loss of function in a CP110-Cep97 pathway promotes the aberrant growth of cilia from centrioles. First, RPE-1 and NIH 3T3 cells, which have been extensively characterized and shown to exhibit normal primary cilia, show a dramatic induction of primary cilia expression upon Cep97 and CP110 depletion in cycling populations. Second, we detected an array of proteins that are among the best-established markers of primary cilia, including the axonemal protein polaris (Michaud and Yoder, 2006), in Cep97 and CP110 depleted cells. In addition, we have used a reciprocal, functional assay, inhibition of cilia assembly in 3T3 cells, to show that we can suppress the formation of these structures by overexpressing CP110, which is normally not expressed during G0. Lastly, we have shown that CP110 is extinguished from basal bodies that become cilia.

Controls must exist in cycling cells to prevent centrioles from acting as basal bodies that nucleate cilium formation because assembly of primary cilia in cycling cells could have catastrophic consequences. First, the failure to resorb cilia prior to entry into mitosis could prevent centrosomes from participating in spindle pole formation and faithful chromosome segregation, leading to elevated genomic instability. Thus, there may be a causal connection between the loss of Cep97 and CP110 at centrosomes, the aberrant formation of cilia that persist into mitosis, and a documented increase in abnormal mitotic spindles and polyploidy. Additional experiments will be required to explain how inappropriate assembly of cilia gives rise to abnormal spindle poles and cytokinesis failure, although it is reasonable to assume that basal body and mitotic spindle organizing functions are incompatible. Moreover, based on the reported requirement for primary cilia in a number of vital signaling pathways, including those involving Shh and PDGFRα, aberrant expression of primary cilia at certain points of the cell cycle may alter the balance between growth stimulatory and inhibitory pathways and thus lead to uncontrolled proliferation. As additional signaling pathways crucial to embryonic development and tumorigenesis are linked to the function of primary cilia, it will become critical to evaluate the effects of aberrant cilia formation on cell growth regulation and normal embryonic development. In light of our findings, Cep97 and CP110 appear to constitute a set of controls that govern the switch from centriolar to basal body function, and they represent a starting point to completely elucidate the pathway that controls this switch in normal cells.

A Role for CP110 and Associated Proteins in Human Ciliary Diseases

Cilia are thought to be essential for determining left-right asymmetry during embryonic development. Defects in

cilia are found in a wide range of human diseases, including polycystic liver, renal disease, and retinal degeneration. Ciliary defects have also been associated with numerous developmental abnormalities, diabetes, and a number of multisymptom disorders, including Joubert Syndrome. This syndrome is marked by photoreceptor degeneration, renal failure, and neurological and cerebellar defects, and recent experiments have mapped the genetic defect to the *Cep290/NPHP6* gene, which encodes a centrosomal protein of unknown function (Sayer et al., 2006; Valente et al., 2006). In some instances, the appearance of disease can be linked directly to a ciliary defect, but in other cases, cilia appear to have a grossly normal appearance and length. Thus, the connections between specific defects in a centrosomal or ciliary protein and disease are largely unknown. Our identification of a pathway linking defects in two centrosomal proteins with aberrant formation of cilia may provide unexpected and exciting new avenues for the discovery of proteins involved in ciliary dysfunction and provide mechanistic insights into the assembly of normal cilia.

EXPERIMENTAL PROCEDURES

Purification and Identification of CP110-Interacting Proteins and Superose 6 Gel Filtration Analysis

Please refer to the Supplemental Experimental Procedures for a detailed description.

Cell Culture, Cell Cycle Synchronization, and FACS Analysis

U2OS, T98G, and NIH 3T3 cells were obtained from ATCC and cultured in DMEM containing 10% fetal bovine serum. RPE-1 hTERT (RPE-1) cells were provided by A. Khodjakov. T98G cells were synchronized as previously described (Chen et al., 2002). U2OS cells were synchronized by 2 mM hydroxyurea treatment for 24 hr followed by release into DMEM with 10% FBS for indicated periods. Propidium iodide staining and FACS analysis were performed as described (Chen et al., 2002). NIH 3T3 cells were transfected with Fugene HD (Roche Applied Science).

Antibodies

To generate rabbit anti-Cep97 antibodies, a glutathione-S-transferase (GST) fusion protein containing amino acids 539–689 of Cep97 was expressed in bacteria and purified to homogeneity. Antibodies against Cep97 were purified by affinity chromatography. Polyclonal rabbit anti-CP110 (Chen et al., 2002), anti-centrin (20H5), anti-calmodulin (Millipore), anti-GFP (Invitrogen), anti-α-tubulin, anti-Acetylated-tubulin, and anti-γ-tubulin (all from Sigma-Aldrich), anti-CG-NAP (gifts from M. Takahashi and Y. Ono) and anti-Polycystin2 (YCC2) antibody (gift of Y. Cai and S. Somlo) were used. Anti-glutamylated-tubulin (GT335) and anti-polaris antibodies were generously provided by C. Janke and B. Yoder, respectively.

RT-PCR

Extraction of total RNA was performed using TRIzol (Invitrogen). SuperScript First-Strand synthesis kit (Invitrogen) was used for first-strand cDNA synthesis. PCR was performed on the resulting cDNA using gene-specific primers for Cep97 and actin. Two independent reactions were performed for each set of primers and linear amplification was assured in each case. Primer sequences are available upon request.

Immunoprecipitation and Immunoblotting

Cells were lysed in ELB buffer at 4°C for 30 min. 2 mg of lysate were incubated with antibody and protein A- or G-Sepharose beads at 4°C for 1 hr. The beads were extensively washed with lysis buffer, and the bound polypeptides were analyzed by SDS-PAGE and immunoblotting. Typically, input lanes contained 50–100 μg of lysate.

Immunofluorescence Microscopy

Indirect immunofluorescence experiments were performed as previously described (Chen et al., 2002). Image acquisition was performed using a Zeiss Axiovert 200 M microscope (63× objective lens, N.A. 1.4, 1.6× Optovar) equipped with a cooled Retiga 2000R CCD (QImaging) and Metamorph Software (Molecular Devices).

RNAi

Small interfering RNA (siRNA) oligonucleotides were obtained from Dharmacon, Inc. Transfection of siRNAs was performed using sImporter (Millipore) per manufacturer's instructions. The siRNA sequences used in this study are shown in the Supplemental Experimental Procedures. We depleted mouse Cep97 and CP110 in 3T3 cells with siRNA Smartpools designed by Dharmacon, Inc.

CP110 and Cep97 Expression Vectors and Mapping Studies

To generate Flag-tagged CP110 and Cep97 fusion proteins, cDNAs were amplified by PCR using Pfu Turbo polymerase (Stratagene) and subcloned into pCBF or pCDEF3, respectively. To generate carboxy-terminally tagged full length Cep97-GFP, *Cep97* was subcloned into mammalian expression vector pEGFP-N1 (Clontech). All constructs were verified by sequencing. Flag-tagged constructs were cotransfected into 293 cells using calcium phosphate. Cells were harvested 48 hr after transfection. Flag beads were incubated with cell extract at 4°C for 2 hr, washed with lysis buffer, and bound proteins were analyzed by SDS-PAGE and immunoblotting.

Supplemental Data

Supplemental Data include Supplemental Experimental Procedures and three figures and can be found with this article online at http://www.cell.com/cgi/content/full/130/4/678/DC1/.

ACKNOWLEDGMENTS

We are most grateful to W. Lane at the Harvard Microchemical Facility for MS analysis of CP110-associated polypeptides and J. Salisbury and C. Janke for anti-centrin and anti-polyglutamylated tubulin antibodies, respectively. We thank E. Nigg (C-Nap1), M. Takahashi and Y. Ono (CG-NAP), Q. Cai and S. Somlo (Polycystin-2), and B. Yoder (polaris) for providing antibodies. We thank A. Khodjakov for providing the RPE-1 cell line and for helpful discussions. We thank all members of the Dynlacht laboratory for constructive advice. This work was supported in part by an Irma T. Hirschl Career Scientist Award to B.D.D., for which he is grateful. A.S. was supported by the DOD Prostate Cancer Research Program (award number W81XWH-07-1-0116). W.Y.T. was supported by NSERC of Canada and Alberta Heritage Foundation for Medical Research postdoctoral fellowships.

Received: November 7, 2006
Revised: April 26, 2007
Accepted: June 13, 2007
Published: August 23, 2007

REFERENCES

Andersen, J.S., Wilkinson, C.J., Mayor, T., Mortensen, P., Nigg, E.A., and Mann, M. (2003). Proteomic characterization of the human centrosome by protein correlation profiling. Nature *426*, 570–574.

Badano, J.L., Mitsuma, N., Beales, P.L., and Katsanis, N. (2006). The Ciliopathies: An Emerging Class of Human Genetic Disorders. Annu. Rev. Genomics Hum. Genet. *7*, 125–148.

Beisson, J., and Wright, M. (2003). Basal body/centriole assembly and continuity. Curr. Opin. Cell Biol. *15*, 96–104.

Bobinnec, Y., Moudjou, M., Fouquet, J.P., Desbruyeres, E., Edde, B., and Bornens, M. (1998). Glutamylation of centriole and cytoplasmic tubulin in proliferating non-neuronal cells. Cell Motil. Cytoskeleton *39*, 223–232.

Cai, Y., Maeda, Y., Cedzich, A., Torres, V.E., Wu, G., Hayashi, T., Mochizuki, T., Park, J.H., Witzgall, R., and Somlo, S. (1999). Identification and characterization of polycystin-2, the PKD2 gene product. J. Biol. Chem. *274*, 28557–28565.

Chen, Z., Indjeian, V.B., McManus, M., Wang, L., and Dynlacht, B.D. (2002). CP110, a cell cycle-dependent CDK substrate, regulates centrosome duplication in human cells. Dev. Cell *3*, 339–350.

Edde, B., Rossier, J., Le Caer, J.P., Desbruyeres, E., Gros, F., and Denoulet, P. (1990). Posttranslational glutamylation of alpha-tubulin. Science *247*, 83–85.

Fry, A.M., Mayor, T., Meraldi, P., Stierhof, Y.D., Tanaka, K., and Nigg, E.A. (1998). C-Nap1, a novel centrosomal coiled-coil protein and candidate substrate of the cell cycle-regulated protein kinase Nek2. J. Cell Biol. *141*, 1563–1574.

Gromley, A., Jurczyk, A., Sillibourne, J., Halilovic, E., Mogensen, M., Groisman, I., Blomberg, M., and Doxsey, S. (2003). A novel human protein of the maternal centriole is required for the final stages of cytokinesis and entry into S phase. J. Cell Biol. *161*, 535–545.

Ishikawa, H., Kubo, A., Tsukita, S., and Tsukita, S. (2005). Odf2-deficient mother centrioles lack distal/subdistal appendages and the ability to generate primary cilia. Nat. Cell Biol. *7*, 517–524.

Keller, L.C., Romijn, E.P., Zamora, I., Yates, J.R., 3rd, and Marshall, W.F. (2005). Proteomic analysis of isolated chlamydomonas centrioles reveals orthologs of ciliary-disease genes. Curr. Biol. *15*, 1090–1098.

Michaud, E.J., and Yoder, B.K. (2006). The primary cilium in cell signaling and cancer. Cancer Res. *66*, 6463–6467.

Pazour, G.J., San Agustin, J.T., Follit, J.A., Rosenbaum, J.L., and Witman, G.B. (2002). Polycystin-2 localizes to kidney cilia and the ciliary level is elevated in orpk mice with polycystic kidney disease. Curr. Biol. *12*, R378–R380.

Quarmby, L.M., and Parker, J.D. (2005). Cilia and the cell cycle? J. Cell Biol. *169*, 707–710.

Rieder, C.L., Jensen, C.G., and Jensen, L.C. (1979). The resorption of primary cilia during mitosis in a vertebrate (PtK1) cell line. J. Ultrastruct. Res. *68*, 173–185.

Salisbury, J.L., Suino, K.M., Busby, R., and Springett, M. (2002). Centrin-2 is required for centriole duplication in mammalian cells. Curr. Biol. *12*, 1287–1292.

Sayer, J.A., Otto, E.A., O'Toole, J.F., Nurnberg, G., Kennedy, M.A., Becker, C., Hennies, H.C., Helou, J., Attanasio, M., Fausett, B.V., et al. (2006). The centrosomal protein nephrocystin-6 is mutated in Joubert syndrome and activates transcription factor ATF4. Nat. Genet. *38*, 674–681.

Sorokin, S.P. (1968). Reconstructions of centriole formation and ciliogenesis in mammalian lungs. J. Cell Sci. *3*, 207–230.

Tsang, W.Y., Spektor, A., Luciano, D.J., Indjeian, V.B., Chen, Z., Salisbury, J.L., Sanchez, I., and Dynlacht, B.D. (2006). CP110 cooperates with two calcium-binding proteins to regulate cytokinesis and genome stability. Mol. Biol. Cell *17*, 3423–3434.

Valente, E.M., Silhavy, J.L., Brancati, F., Barrano, G., Krishnaswami, S.R., Castori, M., Lancaster, M.A., Boltshauser, E., Boccone, L., Al-Gazali, L., et al. (2006). Mutations in CEP290, which encodes a centrosomal protein, cause pleiotropic forms of Joubert syndrome. Nat. Genet. *38*, 623–625.

Wheatley, D.N., Wang, A.M., and Strugnell, G.E. (1996). Expression of primary cilia in mammalian cells. Cell Biol. Int. *20*, 73–81.

Zhao, W.M., Seki, A., and Fang, G. (2006). Cep55, a microtubule-bundling protein, associates with centralspindlin to control the midbody integrity and cell abscission during cytokinesis. Mol. Biol. Cell *17*, 3881–3896.

Zou, C., Li, J., Bai, Y., Gunning, W.T., Wazer, D.E., Band, V., and Gao, Q. (2005). Centrobin: a novel daughter centriole-associated protein that is required for centriole duplication. J. Cell Biol. *171*, 437–445.